Catmull-Clark Subdivision Surfaces with Smoother Extra-ordinary Points

Abstract. The Catmull-Clark subdivision scheme is modified to make the limit surface smoother at the extra-ordinary points.

CR Categories: I.3.5 [Computer Graphics]: Computational Geometry and Object Modeling - curve, surface, solid and object representations;

Keywords: subdivision, Catmull-Clark surfaces, discrete Fourier transform

1 Introduction

Subdivision surfaces have become popular recently in graphical modeling, animation and CAD/CAM because of their capability in capability in modeling/representing complex shape of *arbitrary topology* [5]. See Figure 1(b) for the representation of a ventilation control component with a single subdivision surface. The control mesh of the surface is shown in (a). The ventilation control component has seventeen through holes (handles). Therefore, it can not be represented by a single B-spline or NURBS surface.

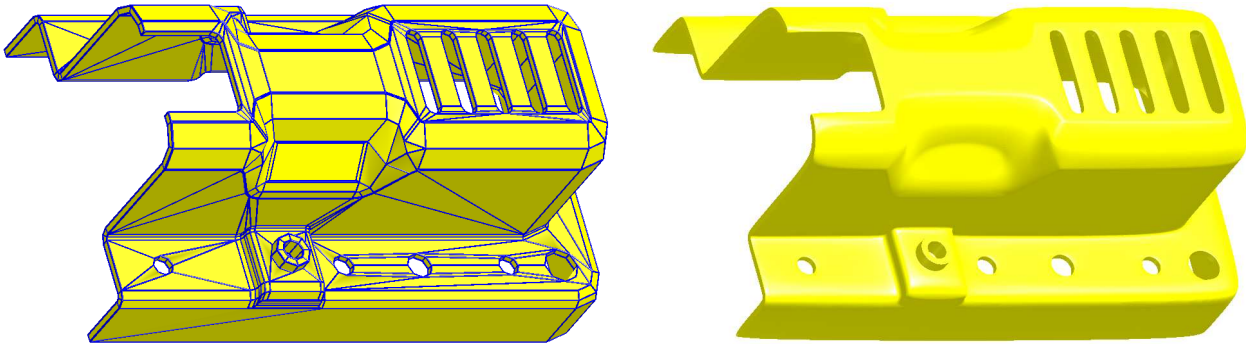

(a) (b)

Figure 1: (a) Control mesh and (b) limit surface of a ventilation control component.

Actually, with the parametrization technique of subdivision surfaces becoming available [10] and with the fact that non-uniform B-spline and NURBS surfaces are special cases of subdivision surfaces becoming known [9], we now know that subdivision surfaces cover both *parametric forms* and *discrete forms*. Parametric forms are good for design and representation; discrete forms are good for machining and tessellation (including FE mesh generation) [1]. Hence, we have a representation scheme that is good potentially for all graphics and CAD/CAM applications.

However, a major problem with the subdivision surfaces remains, i.e., the $C^(2)$ discontinuity at the extra-ordinary points.

In this paper, we will modify the Catmull-Clark subdivision scheme and show that the limit surface is $C^(2)$-continuous everywhere, including the extra-ordinary points.

2 Background

2.1 Catmull-Clark Subdivision Surfaces

Given a control mesh, a *Catmull-Clark subdivision surface* (CCSS) is generated by iteratively refining the control mesh [4]. The iteratively refined control meshes converge to a limit surface. The limit surface is called a *subdivision surface* because the mesh refining process is a generalization of the uniform bicubic B-spline surface subdivision technique. Therefore, CCSSs include uniform B-spline surfaces and piecewise Bézier surfaces as special cases. It is known now that CCSSs include non-uniform B-spline surfaces and NURBS surfaces as special cases as well [9]. The Catmull-Clark mesh refining process is also called the *Catmull-Clark subdivision*, or simply the *subdivision step* subsequently. The *valence* of a mesh vertex is the number of mesh edges adjacent to the vertex. A mesh vertex is called an *extra-ordinary vertex* if its valence is different from four. Vertex $\mathbf{V}$ in Figure 2(a) is an extra-ordinary vertex of valence five.

Mesh faces of a CCSS generated after one iteration of the subdivision step are always quadrilaterals. The number of extra-ordinary vertices remains the same after one iteration of the subdivision step as well. Therefore, after two iterations of the subdivision step, each face has at most one extra-ordinary vertex. We shall assume that all the mesh faces considered subsequently are quadrilaterals and each of them has at most one extra-ordinary vertex.

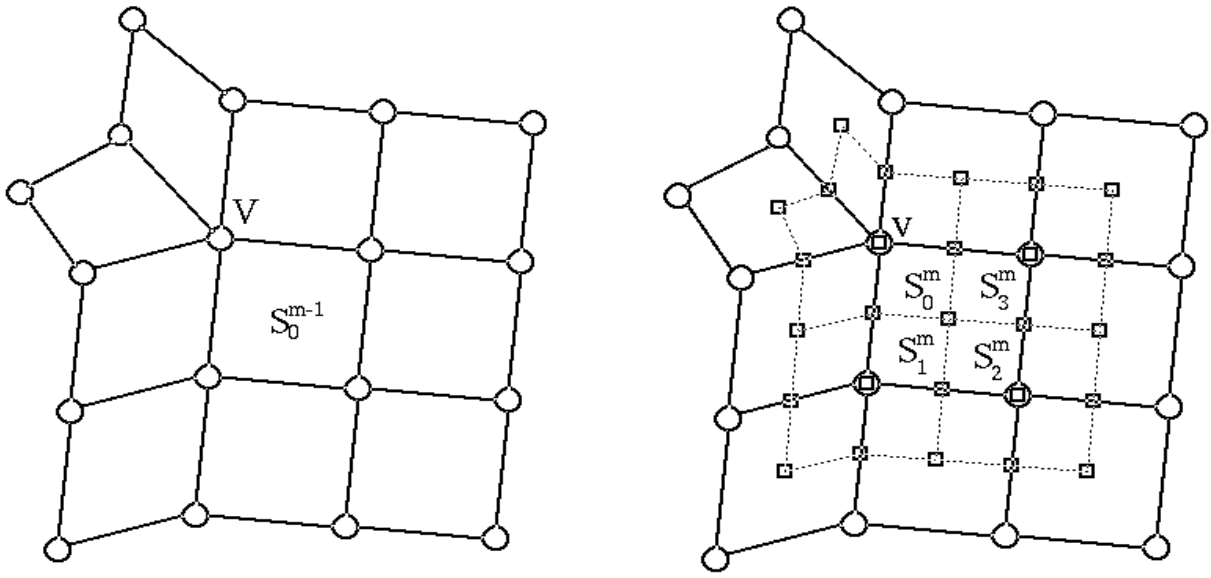

(a) (b)

Figure 2: (a) Control vertices that influence an extra-ordinary patch. (b) New control vertices (small squares) generated after a Catmull-Clark subdivision.

The Catmull-Clark subdivision scheme is the same as the uniform bicubic B-spline surface subdivision on faces not adjacent to an extra-ordinary vertex. Hence, each face not adjacent to an extra-ordinary vertex corresponds to a regular uniform bicubic B-spline patch. Therefore, to evaluate a CCSS, one only needs to develop evaluation techniques for patches corresponding to mesh faces adjacent to extra-ordinary vertices.[1] A mesh face with an extra-ordinary vertex will be called an *extra-ordinary face* and the corresponding patch will be called an *extra-ordinary patch*. In the following, we briefly review the standard evaluation process for an extra-ordinary patch. For the sake of simplicity, a mesh face and the corresponding patch will be treated the same and denoted by the same notation.

Given an extra-ordinary face $\mathbf{S} = \mathbf{S}_0^0$. If the valence of its extra-ordinary vertex is n, then the patch corresponding to this extra-ordinary face is influenced by $2n+8$ control vertices. The control vertices shown

[1] However, it would turn out that the resulting evaluation techniques work for regular patches as well.

in Figure 2(a) are the ones that influence the patch marked with an "$\mathbf{S} = \mathbf{S}_0^{m-1}$". In general, if $\mathbf{S}_0^{m-1}$ is the extra-ordinary subpatch generated after $m-1$ subdivision steps, then by performing a Catmull-Clark subdivision step on the control vertices of $\mathbf{S}_0^{m-1}$, one gets $2n+17$ new control vertices. See Figure 2(b) for the new control vertices generated for patch $\mathbf{S}_0^{m-1}$ shown in (a). These $2n+17$ new control vertices define four subpatches: $\mathbf{S}_b^m$, $b = 0, 1, 2, 3$ (Figure 2(b)). $\mathbf{S}_0^m$ is again an extra-ordinary patch but $\mathbf{S}_1^m$, $\mathbf{S}_2^m$, and $\mathbf{S}_3^m$ are regular uniform bicubic B-spline patches. Iteratively repeat this process, one gets a sequence of regular bicubic B-spline patches $(\mathbf{S}_b^m)$, $m \geq 1$, $b = 1, 2, 3$, a sequence of extra-ordinary patches $(\mathbf{S}_0^m)$, $m \geq 0$, and a sequence of extra-ordinary vertices. The extra-ordinary patches converge to the limit point of the extra-ordinary vertices [7]. The regular bicubic B-spline patches $(\mathbf{S}_b^m)$, $m \geq 1$, $b = 1, 2, 3$, and the limit point of the extra-ordinary vertices form a partition of $\mathbf{S}$.

The regular bicubic B-spline patches $\{\mathbf{S}_b^m\}$, $m \geq 1$, $b = 1, 2, 3$, induce a partition on the unit square $[0,1] \times [0,1]$. The partition is defined by : $\{\mathbf{\Omega}_b^m\}$, $m \geq 1$, $b = 1, 2, 3$, with

$$\begin{aligned} \mathbf{\Omega}_1^m &= [\tfrac{1}{2^m}, \tfrac{1}{2^{m-1}}] \times [0, \tfrac{1}{2^m}], \\ \mathbf{\Omega}_2^m &= [\tfrac{1}{2^m}, \tfrac{1}{2^{m-1}}] \times [\tfrac{1}{2^m}, \tfrac{1}{2^{m-1}}], \\ \mathbf{\Omega}_3^m &= [0, \tfrac{1}{2^m}] \times [\tfrac{1}{2^m}, \tfrac{1}{2^{m-1}}] \end{aligned}$$

(see Figure 3 for an illustration of the partition). For any $(u, v) \in [0,1] \times [0,1]$ but $(u, v) \neq (0, 0)$, there is an $\mathbf{\Omega}_b^m$ that contains (u, v). To find the value of $\mathbf{S}$ at (u, v), first map $\mathbf{\Omega}_b^m$ to the unit square. If (u, v) is mapped to $(\bar{u}, \bar{v})$ by this mapping, then compute the value of $\mathbf{S}_b^m$ at $(\bar{u}, \bar{v})$. The value of $\mathbf{S}$ at $(0, 0)$ is the limit of the extra-ordinary vertices. For the convenience of subsequent reference, the above partition will be called an Ω-*partition* of the unit square.

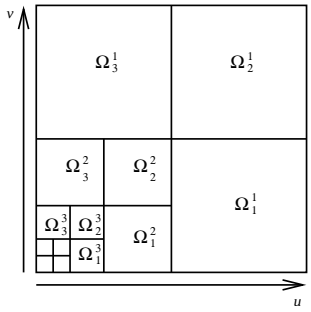

Figure 3: Ω-partition of the unit square.

3 Modified Catmull-Clark Subdivision Scheme

The above standard subdivision/evaluation technique for an extra-ordinary patch has a problem: the resulting limit surface would not be C^2 continuous at the extra-ordinary points [2, 3]. This is because the surface would oscillate when it is close to an extra-ordinary point. This is especially true when the valance of the extra-ordinary point is large. This is because the way a face point is defined. A face point is defined as the average of its face vertices. It does not get influence from its neighboring faces at all. When the shape of a face gets squeezed by its neighboring faces, the face point get squeezed as well. One can avoid the squeezing effect by averaging a face point with adjacent face points. However, when one does the averaging, one needs to ensure the resulting limit surface still interpolates vertices of the original limit surface so that the new limit surface resembles the original limit surface. A technique is presented below.

3.1 Basic Concept

In Figure 2(b), we don't define $\mathbf{S}_b^m$, $b = 1, 2, 3$, immediately. We will perform one more (standard) subdivision to get new control points such as the ones marked with a small diamond in Figure 3(a). At

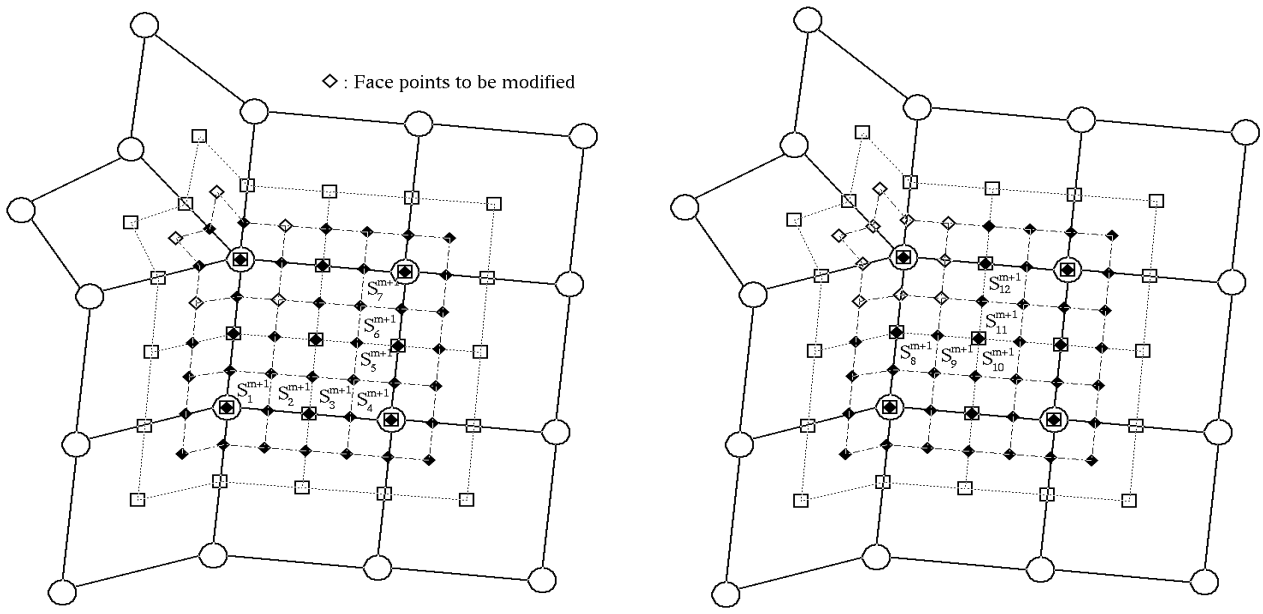

(a) (b)

Figure 4: (a) Subpatches 1-7 and their defining control vertices (solid diamonds). (b) Subpatches 8-12 and defining control vertices after the modification of the faces points and the edge points (hollow diamonds).

this point, we define subpatches $\mathbf{S}_b^{m+1}$, $b = 1, 2, ..., 7$. Once these subpatches have been defined, we modify the face points (the one marked with a hollow diamond in Figure 4(a)) and related edge points and then define subpatches $\mathbf{S}_b^{m+1}$, $b = 8, 9, ..., 12$.

If the control points are labeled according to the scheme shown in Figure 5, then the face point is modified as follows:

$$\bar{\mathbf{F}}_j^{m+1} = (1-\delta)\ \left(\frac{\mathbf{F}_{j-1}^{m+1} + \mathbf{F}_{j+1}^{m+1}}{2}\right) + \delta\ \mathbf{F}_j^{m+1} \tag{1}$$

where $\mathbf{F}_i^{m+1}$ and $\bar{\mathbf{F}}_i^{m+1}$ are face points before and after the modification, respectively, and δ is a non-negative number between 0 and 1. The purpose of the modification process is to blend each face point with its adjacent face points so that the face points would lie in the same plane as they converge to the extra-ordinary point.

Since the definition of an edge point depends on adjacent face points, this means related edge points should be modified as well. If we use $\bar{\mathbf{E}}_j^{m+1}$ to represent an edge point after modification then we have

$$\bar{\mathbf{E}}_j^{m+1} = \left(\frac{\mathbf{V} + \mathbf{E}_j^m}{2} + \frac{\bar{\mathbf{F}}_{j-1}^{m+1} + \bar{\mathbf{F}}_j^{m+1}}{2}\right)/2$$

It is easy to see that the new expressions of these face points and edge points are

$$\bar{\mathbf{F}}_j^{m+1} = \tfrac{1}{4}\mathbf{V} + \tfrac{1-\delta}{8}\mathbf{E}_{j-1}^m + \tfrac{1+\delta}{8}\mathbf{E}_j^m + \tfrac{1+\delta}{8}\mathbf{E}_{j+1}^m + \tfrac{1-\delta}{8}\mathbf{E}_{j+2}^m$$

$$+ \tfrac{1-\delta}{8}\mathbf{F}_{j-1}^m + \tfrac{\delta}{4}\mathbf{F}_j^m + \tfrac{1-\delta}{8}\mathbf{F}_{j+1}^m$$

and

$$\bar{\mathbf{E}}_j^{m+1} = \tfrac{3}{8}\mathbf{V} + \tfrac{1-\delta}{32}\mathbf{E}_{j-2}^m + \tfrac{1}{16}\mathbf{E}_{j-1}^m + \tfrac{5+\delta}{16}\mathbf{E}_j^m + \tfrac{1}{16}\mathbf{E}_{j+1}^m + \tfrac{1-\delta}{32}\mathbf{E}_{j+2}^m$$

$$+ \tfrac{1-\delta}{32}\mathbf{F}_{j-2}^m + \tfrac{1+\delta}{32}\mathbf{F}_{j-1}^m + \tfrac{1+\delta}{32}\mathbf{F}_j^m + \tfrac{1-\delta}{32}\mathbf{F}_{j+1}^m,$$

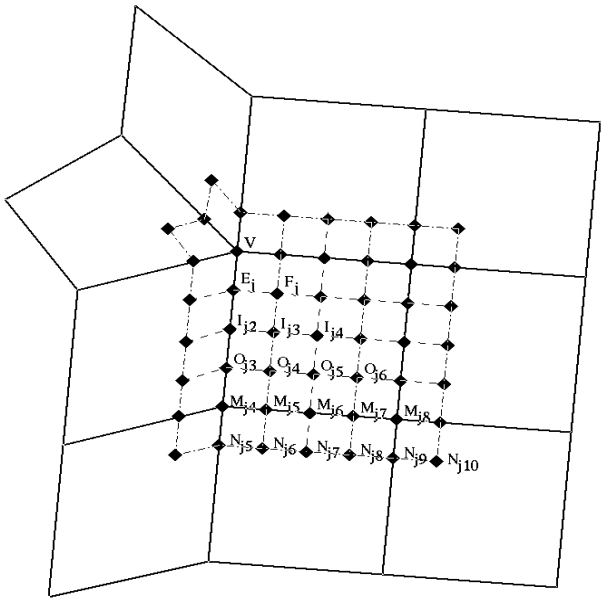

Figure 5: Labeling of the control vertices around an extra-ordinary vertex.

respectively.

Once the face points and the edge points are modified, they are used to define the subpatches $\mathbf{S}_b^{m+1}$, $b = 8, 9, ..., 12$, as the ones shown in Figure 4(b). These subpataches share a common boundary with the subpatches $\mathbf{S}_b^{m+1}$, $b = 1, 2, ..., 7$. It is easy to see that they satisfy C^2-continuity on this common boundary.

By repeatedly applying this process to the remaining subpatches, we fill up the domain with C^2-continous subpatches, with the exception of the endpoint $(0, 0)$.

Note that the above modification process does not affect the location of the vertex point $\mathbf{V}^{m+1}$. This follows the observation that

$$\sum_{i=1}^{n} \bar{\mathbf{F}}_i^{m+1} \;=\; \sum_{i=1}^{n} \mathbf{F}_i^{m+1} \qquad and \qquad \sum_{i=1}^{n} \bar{\mathbf{E}}_i^{m+1} \;=\; \sum_{i=1}^{n} \mathbf{E}_i^{m+1}$$

Therefore, the limit point of the extra-ordinary points remains the same.

4 Parametrization of an Extra-Ordinary Patch

The parametrization of an extra-ordinary patch under the modified subdivision scheme is slightly different from the standard approach shown in Section 2. The standard approach uses the partition scheme shown in Figure 3 for the parameter space while the new approach uses the partition scheme shown in Figure 6 to partition the parameter space. However, for simplicity of terminology, we will refer both partition schemes as an Ω-partition.

Let $\{\mathbf{\Omega}_b^m\}$, $m \geq 1$, $b = 1, 2, ..., 12$, be an Ω-partition of the unit square as the one shown in Figure 6. For any $(u, v) \in [0, 1] \times [0, 1]$ but $(u, v) \neq (0, 0)$, first find the $\mathbf{\Omega}_b^m$ that contains (u, v). m and b can be computed as follows:

$$m(u, v) = min\{\lfloor log_{\frac{1}{2}} u \rfloor, \lfloor log_{\frac{1}{2}} v \rfloor\} \ ,$$

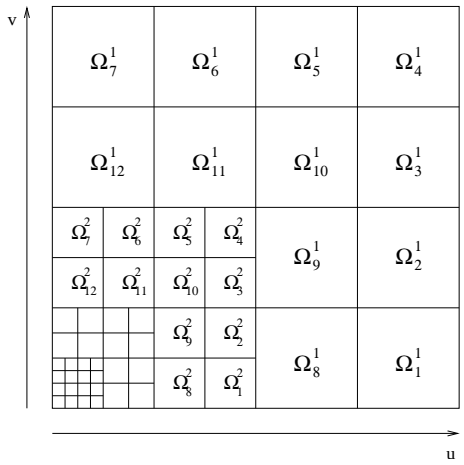

Figure 6: Ω-partition of the unit square for the new approach.

$$b(u,v) = \begin{cases} 1, & if \;\; 2^{m+1}u \in [3,4) \;\; and \;\; 2^{m+1}v \in [0,1) \\ 2, & if \;\; 2^{m+1}u \in [3,4) \;\; and \;\; 2^{m+1}v \in [1,2) \\ 3, & if \;\; 2^{m+1}u \in [3,4) \;\; and \;\; 2^{m+1}v \in [2,3) \\ 4, & if \;\; 2^{m+1}u \in [3,4) \;\; and \;\; 2^{m+1}v \in [3,4) \\ 5, & if \;\; 2^{m+1}u \in [2,3) \;\; and \;\; 2^{m+1}v \in [3,4) \\ 6, & if \;\; 2^{m+1}u \in [1,2) \;\; and \;\; 2^{m+1}v \in [3,4) \\ 7, & if \;\; 2^{m+1}u \in [0,1) \;\; and \;\; 2^{m+1}v \in [3,4) \\ 8, & if \;\; 2^{m+1}u \in [2,3) \;\; and \;\; 2^{m+1}v \in [0,1) \\ 9, & if \;\; 2^{m+1}u \in [2,3) \;\; and \;\; 2^{m+1}v \in [1,2) \\ 10, & if \;\; 2^{m+1}u \in [2,3) \;\; and \;\; 2^{m+1}v \in [2,3) \\ 11, & if \;\; 2^{m+1}u \in [1,2) \;\; and \;\; 2^{m+1}v \in [2,3) \\ 12, & if \;\; 2^{m+1}u \in [0,1) \;\; and \;\; 2^{m+1}v \in [2,3) \end{cases}$$

Then map this $\mathbf{\Omega}_b^m$ to the unit square with the following mapping:

$$(x,y) \;\rightarrow\; (\phi(x),\phi(y))$$

where

$$\phi(t) = \begin{cases} 2^{m+1}t, & if \;\; 2^{m+1}t < 1 \\ 2^{m+1}t - 1, & if \;\; 1 \le 2^{m+1}t < 2 \\ 2^{m+1}t - 2, & if \;\; 2 \le 2^{m+1}t < 3 \\ 2^{m+1}t - 3, & if \;\; 3 \le 2^{m+1}t < 4 \end{cases} \tag{2}$$

If $(\bar{u},\bar{v}) = (\phi(u),\phi(v))$ is the image of (u,v) under this mapping, then the value of the extra-ordinary patch at this point, denoted $\mathbf{S}(u,v)$, can be expressed as:

$$\mathbf{S}(u,v) = (W(\bar{u},\bar{v}))^T \, M G_{m,b} \tag{3}$$

where $G_{m,b}$ is the (16×1) control vertex vector of $\mathbf{S}_b^m$ (the subpatch defined on Ω_b^m), $W(u,v)$ is a vector containing the 16 power basis functions:

$$(W(u,v))^T = [1, u, v, u^2, uv, v^2, u^3, u^2v, uv^2, v^3, u^3v, u^2v^2, uv^3, u^3v^2, u^2v^3, u^3v^3], \tag{4}$$

M is the coefficient matrix of a regular B-spline patch (see Appendix A for the computation of M), and $(W(u,v))^T$ is the transpose of $W(u,v)$. An important observation is, $(W(\bar{u},\bar{v}))^T$ can be expressed as the product of $(W(u,v))^T$ and two matrices:

$$(W(\bar{u},\bar{v}))^T = (W(u,v))^T \mathrm{K}^{m+1} \mathrm{D_b}$$

where K is a diagonal matrix

$$\mathrm{K} = Diag(1, 2, 2, 4, 4, 4, 8, 8, 8, 8, 16, 16, 16, 32, 32, 64)$$

and $\mathrm{D_b}$ is an upper triangular matrix depending on b only. $\mathrm{D_b}$ can be obtained by replacing $\bar{u},\ \bar{v}$ in $W(\bar{u}, \bar{v})$ with $\phi(u),\ \phi(v)$ defined in Eq. (2). They are shown in Appendix B. Therefore, we have

$$\mathbf{S}(u, v) = (W(u, v))^T \mathrm{K^{m+1}D_bM}G_{m,b}.$$

4.1 Calculation of Control Points

The computation of the control vertices of $\mathbf{S}_b^m$ involves several matrices and it also depends on the value of m. A and $\bar{\mathrm{A}}$ [10]. $\bar{\mathrm{A}}$ is a $(2n + 17) \times (2n + 8)$ matrix, representing the subdivision process shown in Figure 2(b). A is a $(2n + 8) \times (2n + 8)$ submatrix of $\bar{\mathrm{A}}$, representing the process of mapping the $2n + 8$ control vertices of the given extra-ordinary patch to the $2n + 8$ control vertices of its extra-ordinary subpatch. Let

$$G = [\mathbf{V}, \mathbf{E}_1, \cdots, \mathbf{E}_n, \mathbf{F}_1, \cdots, \mathbf{F}_n, \mathbf{I}_1, \cdots, \mathbf{I}_7]$$

then G (See Fig. 2(a) for its labelling) is the column vector representing the control vertices of $\mathbf{S}$. By applying A to G $(m - 1)$ times we get the $2n + 8$ control vertices of the extra-ordinary subpatch $\mathbf{S}_{m-1,0}$. Now by applying $\bar{\mathrm{A}}$ to the control vertices of $\mathbf{S}_{m-1,0}$ (represented as G_{m-1}), we get $2n + 17$ new control points which include the $2n + 8$ control vertices of $\mathbf{S}_{m,0}$. Let $\bar{G}_m$ be the column vector representation of these $2n + 17$ vertices, we have $\bar{G}_m = \bar{\mathrm{A}}G_{m-1} = \bar{\mathrm{A}}\mathrm{A}^{m-1}G$. Then by multiplying $\bar{G}_m$ with an appropriate "picking" matrix P_b, we get the control vertices of the subpatch $\mathbf{S}_{m,b}$: $G_{m,b} = \mathrm{P}_b\bar{G}_m = \mathrm{P}_b\bar{\mathrm{A}}\mathrm{A}^{m-1}G$. Hence we have

$$\mathbf{S}(u, v) = W^T(u, v)\mathrm{K^m D_bMP}_b\bar{\mathrm{A}}\mathrm{A}^{m-1}G. \tag{5}$$

This is a parametrization of an extra-ordinary patch. However, this is a costly process to use because it involves $m - 1$ multiplications of the $(2n + 8) \times (2n + 8)$ matrix A. In the next section, we will present an efficient approach to calculate $G_{m,b}$ for any b and m.

A Computation of Coefficient Matrix M

A uniform cubic B-spline surface patch $\mathbf{S}(u, v)$ is defined as

$$\mathbf{S}(u, v) \ = \ \sum_{i=0}^{3} N_i(u) \sum_{j=0}^{3} N_j(v)\mathbf{P}_{i,j}$$

where $N_i(t)$ are uniform B-spline basis functions and $\mathbf{P}_{i,j}$ are control points. By arranging all the control points in a 16×1 vector G as follows

$$G \ = \ [\mathbf{P}_{0,0}, \ldots, \mathbf{P}_{0,3}, \mathbf{P}_{1,0}, \ldots, \mathbf{P}_{1,3}, \mathbf{P}_{2,0}, \ldots, \mathbf{P}_{2,3}, \mathbf{P}_{3,0}, \ldots, \mathbf{P}_{3,3}]^T$$

$\mathbf{S}(u, v)$ can also be expressed as

$$\mathbf{S}(u, v) \ = \ (W(u, v))^T MG$$

where $W(u, v)$ is defined in eq. (4) and M is a 16×16 coefficient matrix. To compute M, note that the k-th column of M, denoted $\mathbf{M}_k$, corresponds to $N_i(u)$ and $N_j(v)$ where

$$i \ = \ (k - 1) \ \% \ 4 \qquad and \qquad j \ = \ (k - 1) \bmod 4$$

Hence, to compute $\mathbf{M}_k$, we need to compute i and j and then carry out the mulplication of $N_i(u)$ and $N_j(v)$. Without loss of generality, in the following, we will show the computation process of M_0 only.

Recall that $N_i(t)$ are defined as follows

$$[N_0(t), N_1(t), N_2(t), N_3(t)] \;=\; \frac{1}{6}\,\mathbf{T}^T\,[\mathbf{Q}_0, \mathbf{Q}_1, \mathbf{Q}_2, \mathbf{Q}_3] \;=\; \frac{1}{6}\,\mathbf{T}^T \begin{bmatrix} 1 & 4 & 1 & 0 \\ -3 & 0 & 3 & 0 \\ 3 & -6 & 3 & 0 \\ -1 & 3 & -3 & 1 \end{bmatrix}$$

where $\mathbf{T} \;=\; [1, t, t^2, t^3]^T$. Hence,

$$N_0(u)N_0(v) = N_0(u)(N_0(v))^T = \frac{1}{36}\mathbf{U}^T\mathbf{Q}_0(\mathbf{Q}_0)^T\mathbf{V} = \frac{1}{36}W(u,v)\mathbf{M}_1$$

The relationship between $\mathbf{M}_1$ and $\mathbf{Q}_0(\mathbf{Q}_0)^T$ is as follows. If $Q = \mathbf{Q}_0(\mathbf{Q}_0)^T$ then we have

$$\begin{array}{llll} \mathbf{M}_{1,1} = Q_{1,1} & \mathbf{M}_{1,2} = Q_{2,1} & \mathbf{M}_{1,3} = Q_{1,2} & \mathbf{M}_{1,4} = Q_{3,1} \\ \mathbf{M}_{1,5} = Q_{2,2} & \mathbf{M}_{1,6} = Q_{1,3} & \mathbf{M}_{1,7} = Q_{4,1} & \mathbf{M}_{1,8} = Q_{3,2} \\ \mathbf{M}_{1,9} = Q_{2,3} & \mathbf{M}_{1,10} = Q_{1,4} & \mathbf{M}_{1,11} = Q_{4,2} & \mathbf{M}_{1,12} = Q_{3,3} \\ \mathbf{M}_{1,13} = Q_{2,4} & \mathbf{M}_{1,14} = Q_{4,3} & \mathbf{M}_{1,15} = Q_{3,4} & \mathbf{M}_{1,16} = Q_{4,4} \end{array}$$

The entire coefficient matrix is given below.

$$M \;=\; \begin{bmatrix} 1 & 4 & 1 & 0 & 4 & 16 & 4 & 0 & 1 & 4 & 1 & 0 & 0 & 0 & 0 & 0 \\ -3 & -12 & -3 & 0 & 0 & 0 & 0 & 0 & 3 & 12 & 3 & 0 & 0 & 0 & 0 & 0 \\ -3 & 0 & 3 & 0 & -12 & 0 & 12 & 0 & -3 & 0 & 3 & 0 & 0 & 0 & 0 & 0 \\ 3 & 12 & 3 & 0 & -6 & -24 & -6 & 0 & 3 & 12 & 3 & 0 & 0 & 0 & 0 & 0 \\ 9 & 0 & -9 & 0 & 0 & 0 & 0 & 0 & -9 & 0 & 9 & 0 & 0 & 0 & 0 & 0 \\ 3 & -6 & 3 & 0 & 12 & -24 & 12 & 0 & 3 & -6 & 3 & 0 & 0 & 0 & 0 & 0 \\ -1 & -4 & -1 & 0 & 3 & 12 & 3 & 0 & -3 & -12 & -3 & 0 & 1 & 4 & 1 & 0 \\ -9 & 0 & 9 & 0 & 18 & 0 & -18 & 0 & -9 & 0 & 9 & 0 & 0 & 0 & 0 & 0 \\ -9 & 18 & -9 & 0 & 0 & 0 & 0 & 0 & 9 & -18 & 9 & 0 & 0 & 0 & 0 & 0 \\ -1 & 3 & -3 & 1 & -4 & 12 & -12 & 4 & -1 & 3 & -3 & 1 & 0 & 0 & 0 & 0 \\ 3 & 0 & -3 & 0 & -9 & 0 & 9 & 0 & 9 & 0 & -9 & 0 & -3 & 0 & 3 & 0 \\ 9 & -18 & 9 & 0 & -18 & 36 & -18 & 0 & 9 & -18 & 9 & 0 & 0 & 0 & 0 & 0 \\ 3 & -9 & 9 & -3 & 0 & 0 & 0 & 0 & -3 & 9 & -9 & 3 & 0 & 0 & 0 & 0 \\ -3 & 6 & -3 & 0 & 9 & -18 & 9 & 0 & -9 & 18 & 9 & 0 & 3 & -6 & 3 & 0 \\ -3 & 9 & -9 & 3 & 6 & -18 & 18 & -6 & -3 & 9 & -9 & 3 & 0 & 0 & 0 & 0 \\ 1 & -3 & 9 & -1 & -3 & 9 & -9 & 3 & 3 & -9 & 9 & -3 & -1 & 3 & -3 & 1 \end{bmatrix}$$

B Computation of D_b

The general form of $W(\bar{u},\bar{v})$ is $W(\bar{u},\bar{v}) = W(2^{m+1}u+i,\ 2^{m+1}v+j)$ for some $-3 \le i,j \le 0$. Hence, the general form of D_b is

$$D_b = \begin{bmatrix}
1 & i & j & i^2 & ij & j^2 & i^3 & i^2j & ij^2 & j^3 & i^3j & i^2j^2 & ij^3 & i^3j^2 & i^2j^3 & i^3j^3 \\
 & 1 & 0 & 2i & j & 0 & 3i^2 & 2ij & j^2 & 0 & 3i^2j & 2ij^2 & j^3 & 3i^2j^2 & 2ij^3 & 3i^2j^3 \\
 & & 1 & 0 & i & 2j & 0 & i^2 & 2ij & 3j^2 & i^3 & 2i^2j & 3ij^2 & 2i^3j & 3i^2j^2 & 3i^3j^2 \\
 & & & 1 & 0 & 0 & 3i & j & 0 & 0 & 3ij & j^2 & 0 & 3ij^2 & j^3 & 3ij^3 \\
 & & & & 1 & 0 & 0 & 2i & 2j & 0 & 3i^2 & 4ij & 3j^2 & 6i^2j & 6ij^2 & 9i^2j^2 \\
 & & & & & 1 & 0 & 0 & i & 3j & 0 & i^2 & 3ij & i^3 & 3i^2j & 3i^3j \\
 & & & & & & 1 & 0 & 0 & 0 & j & 0 & 0 & j^2 & 0 & j^3 \\
 & & & & & & & 1 & 0 & 0 & 3i & 2j & 0 & 6ij & 3j^2 & 9ij^2 \\
 & & & & & & & & 1 & 0 & 0 & 2i & 3j & 3i^2 & 6ij & 9i^2j \\
 & & & & & & & & & 1 & 0 & 0 & i & 0 & i^2 & i^3 \\
 & & & & & & & & & & 1 & 0 & 0 & 2j & 0 & 3j^2 \\
 & & & & & & & & & & & 1 & 0 & 3i & 3j & 9ij \\
 & & & & & & & & & & & & 1 & 0 & 2i & 3i^2 \\
 & & & & & & & & & & & & & 1 & 0 & 3j \\
 & & & & & & & & & & & & & & 1 & 3i \\
 & & & & & & & & & & & & & & & 1
\end{bmatrix}$$

Consequently, for D_1 $(i=-3,\ j=0)$ we have

$$D_1 = \begin{bmatrix}
1 & -3 & 0 & 9 & 0 & 0 & -27 & 0 & 0 & 0 & 0 & 0 & 0 & 0 & 0 & 0 \\
 & 1 & 0 & -6 & 0 & 0 & 27 & 0 & 0 & 0 & 0 & 0 & 0 & 0 & 0 & 0 \\
 & & 1 & 0 & -3 & 0 & 0 & 9 & 0 & 0 & -27 & 0 & 0 & 0 & 0 & 0 \\
 & & & 1 & 0 & 0 & -9 & 0 & 0 & 0 & 0 & 0 & 0 & 0 & 0 & 0 \\
 & & & & 1 & 0 & 0 & -6 & 0 & 0 & 27 & 0 & 0 & 0 & 0 & 0 \\
 & & & & & 1 & 0 & 0 & -3 & 0 & 0 & 9 & 0 & -27 & 0 & 0 \\
 & & & & & & 1 & 0 & 0 & 0 & 0 & 0 & 0 & 0 & 0 & 0 \\
 & & & & & & & 1 & 0 & 0 & -9 & 0 & 0 & 0 & 0 & 0 \\
 & & & & & & & & 1 & 0 & 0 & -6 & 0 & 27 & 0 & 0 \\
 & & & & & & & & & 1 & 0 & 0 & -3 & 0 & 9 & -27 \\
 & & & & & & & & & & 1 & 0 & 0 & 0 & 0 & 0 \\
 & & & & & & & & & & & 1 & 0 & -9 & 0 & 0 \\
 & & & & & & & & & & & & 1 & 0 & -6 & 27 \\
 & & & & & & & & & & & & & 1 & 0 & 0 \\
 & & & & & & & & & & & & & & 1 & -9 \\
 & & & & & & & & & & & & & & & 1
\end{bmatrix}$$

Other D_b can be computed similarly.

C Representation and Eigenstructure of T_ω

Each T_ω, $0 \le \omega \le N-1$, is a 7×7 matrix of the following form:

$$\mathrm{T}_\omega = \begin{bmatrix}
\bar{\alpha}_\omega & \beta_N\delta_\omega & \gamma_N\delta_\omega & 0 & 0 & 0 & 0 \\
\frac{3\delta_\omega}{8} & \frac{3+c_\omega}{8} & \frac{1+a^*_\omega}{16} & 0 & 0 & 0 & 0 \\
\frac{\delta_\omega}{4} & \frac{1+a_\omega}{4} & \frac{1}{4} & 0 & 0 & 0 & 0 \\
\frac{\delta_\omega}{16} & \frac{6+a^*_\omega}{16} & \frac{3a^*_\omega}{8} & \frac{1}{16} & \frac{1}{16} & 0 & 0 \\
\frac{3\delta_\omega}{32} & \frac{18+c_\omega}{32} & \frac{3(1+a^*_\omega)}{32} & \frac{1}{64} & \frac{3}{32} & \frac{1}{64} & 0 \\
\frac{\delta_\omega}{16} & \frac{6+a_\omega}{16} & \frac{3}{8} & 0 & \frac{1}{16} & \frac{1}{16} & 0 \\
\frac{\delta_\omega}{64} & \frac{3(1+a_\omega)}{32} & \frac{9}{16} & \frac{3a_\omega}{32} & \frac{1+a_\omega}{64} & \frac{3}{32} & \frac{1}{64}
\end{bmatrix}$$

where $\bar{\alpha}_\omega = 1 - \delta_\omega(\beta_N + \gamma_N)$, and

$$\delta_\omega = \begin{cases} 1\ , & \text{if } \omega = 0 \\ 0\ , & \text{otherwise} \end{cases}$$

The eigenvalues of T_ω are 1,ξ_ω, $\xi_\omega^{'}$, $\frac{1}{8}$,$\frac{1}{16}$,$\frac{1}{32}$ and $\frac{1}{64}$, where $\xi_\omega, \xi_\omega^{'}$ are roots of the quadratic equation:

$$\xi^2 - \frac{8\bar{\alpha}_\omega + c_\omega - 3}{8}\xi + (\frac{1}{16} - \frac{\beta_n \delta_\omega}{8}) = 0\ .$$

The corresponding matrix of eigenvectors is

$$\mathrm{X}_\omega = [\eta_\omega^1, \eta_\omega, \eta_\omega', \eta_\omega^{1/8}, \eta_\omega^{1/16}, \eta_\omega^{1/32}, \eta_\omega^{1/64}]$$

where

$$\begin{array}{lcl} \eta_\omega^1 & = & [1, \delta_\omega, \delta_\omega, \delta_\omega, \delta_\omega, \delta_\omega, \delta_\omega]^T \\ \eta_\omega^{1/8} & = & [0, 0, 0, 1, 1, 1, 1 + a_\omega]^T \\ \eta_\omega^{1/16} & = & [0, 0, 0, 1, 0, -1, 2(a_\omega - 1)]^T \\ \eta_\omega^{1/32} & = & [0, 0, 0, 2, -1, 2, 11(1 + a_\omega)]^T \\ \eta_\omega^{1/64} & = & [0, 0, 0, 0, 0, 0, 1]^T \end{array}$$

and

$$\eta_0 = \begin{bmatrix} 16\xi^2 - 12\xi + 1 \\ 6\xi - 1 \\ 4\xi + 1 \\ \frac{(256\xi^3 + 864\xi^2 - 30\xi - 5)}{(8\xi - 1)(32\xi - 1)} \\ \frac{(384\xi^3 + 800\xi^2 - 104\xi + 5)}{(8\xi - 1)(32\xi - 1)} \\ \frac{(256\xi^3 + 864\xi^2 - 30\xi - 5)}{(8\xi - 1)(32\xi - 1)} \\ \frac{(4096\xi^4 + 55424\xi^3 + 10224\xi^2 - 1364\xi - 25)}{(8\xi - 1)(32\xi - 1)(64\xi - 1)} \end{bmatrix}$$

with $\xi = \xi_0$, η_0' is given by a similr vector, ξ_0 being changed to ξ_0'. When $\omega \neq 0$, we have

$$\eta_\omega = \begin{bmatrix} 0 \\ 4\xi - 1 \\ 1 + a_\omega \\ \frac{2(400\xi^2 + 36\xi - 13)}{(16\xi - 1)(32\xi - 1)} + \frac{4\xi + 5}{16\xi - 1} a_\omega^* \\ \frac{2(4\xi - 1)(4\xi + 13)}{32\xi - 1} \\ \frac{2(400\xi^2 + 36\xi - 13)}{(16\xi - 1)(32\xi - 1)} + \frac{4\xi + 5}{16\xi - 1} a_\omega \\ \frac{10(1280\xi^3 + 2128\xi^2 - 56\xi - 13)}{(16\xi - 1)(32\xi - 1)(64\xi - 1)}(1 + a_\omega) \end{bmatrix}$$

where $\xi = \xi_\omega$. $\eta_\omega^{'}$ is given by a similr vector, ξ_ω being changed to $\xi_\omega^{'}$.

To decompose T_ω as $\mathrm{X}_\omega \Lambda_\omega \mathrm{X}_\omega^{-1}$, where Λ_ω is the diagonal matrix of eigenvalues of T_ω, one also needs to compute X_ω^{-1}. For simplicity of notations, we use r_k and s_k to represent the k-th row of η_ω and η_ω', respectively. Then X_ω^{-1} can be written as follows:

$$\mathrm{X}_\omega^{-1} = \begin{bmatrix} \mathrm{R}_\omega & \mathbf{0} \\ \mathrm{B}_\omega \mathrm{R}_\omega & \mathrm{K}_\omega \end{bmatrix}_{7 \times 7}$$

where

$$\mathrm{R}_\omega = \frac{1}{k_0} \begin{bmatrix} t_{12} & \delta_\omega t_{20} & \delta_\omega t_{01} \\ \delta_\omega(s_1 - s_2) & s_2 - \delta_\omega s_0 & \delta_\omega s_0 - s_1 \\ \delta_\omega(r_2 - r_1) & \delta_\omega r_0 - r_2 & r_1 - \delta_\omega r_0 \end{bmatrix}_{3 \times 3}$$

$$\mathrm{B}_\omega = \frac{-1}{6}\begin{bmatrix} 6\delta_\omega & r_3+4r_4+r_5 & s_3+4s_4+s_5 \\ 0 & 3(r_3-r_5) & 3(s_3-s_5) \\ 0 & r_3-2r_4+r_5 & s_3-2s_4+s_5 \\ -6\delta_\omega & -6k_1 & -6k_2 \end{bmatrix}_{4\times 3}$$

$$\mathrm{K}_\omega = \begin{bmatrix} \frac{1}{6} & \frac{2}{3} & \frac{1}{6} & 0 \\ \frac{1}{2} & 0 & -\frac{1}{2} & 0 \\ \frac{1}{6} & -\frac{1}{3} & \frac{1}{6} & 0 \\ -(3a_\omega+1) & 3a_\omega+3 & -(a_\omega+3) & 1 \end{bmatrix}_{4\times 4}$$

with

$$\begin{aligned} t_{ij} &= r_i s_j - r_j s_i, \\ k_0 &= t_{12} + \delta_\omega t_{01} + \delta_\omega t_{20}, \\ k_1 &= (3a_\omega+1)r_3 - (3a_\omega+3)r_4 + (a_\omega+3)r_5 - r_6, \\ k_2 &= (3a_\omega+1)s_3 - (3a_\omega+3)s_4 + (a_\omega+3)s_5 - s_6. \end{aligned}$$

D Eigenvalues of T

Evan though each diagonal block of T has seven eigenvalues, however, since five of them are common eigenvalues (i.e., 1, 1/8, 1/16, 1/32 and 1/64) and the other eigenvalues $\{\ \xi_\omega, \xi_\omega^{'}\}$, $0 \le \omega \le N-1$, satisfy the condition $\xi_\omega = \xi_{N-\omega}$, the number of different eigenvalues of T is $N+6$ only. When N is odd, these eigenvalues are:

$$1, \xi_0, \xi_0^{'}, \ldots, \xi_{\lfloor \frac{N}{2} \rfloor - 1}, \xi_{\lfloor \frac{N}{2} \rfloor - 1}^{'}, \xi_{\lfloor \frac{N}{2} \rfloor}, \xi_{\lfloor \frac{N}{2} \rfloor}^{'}, \frac{1}{8}, \frac{1}{16}, \frac{1}{32}, \frac{1}{64}$$

When N is even, these eigenvalues are:

$$1, \xi_0, \xi_0^{'}, \ldots, \xi_{\frac{N}{2}-1}, \xi_{\frac{N}{2}-1}^{'}, \xi_{\frac{N}{2}}, \frac{1}{8}, \frac{1}{16}, \frac{1}{32}, \frac{1}{64}$$

These eigenvalues are labelled as follows:

$$\begin{aligned} &\lambda_0 = 1, \\ &\lambda_{2j+1} = \xi_j \ ; \ \ \lambda_{2(j+1)} = \xi_j^{'} \ , \quad j = 0, 1, \cdots, \lfloor \tfrac{N}{2} \rfloor - 1 \\ &\lambda_{2\lfloor \frac{N}{2} \rfloor + 1} = \xi_{\lfloor \frac{N}{2} \rfloor}, \\ &\lambda_{2\lfloor \frac{N}{2} \rfloor + 2} = \xi_{\lfloor \frac{N}{2} \rfloor}^{'} \ , \quad \text{if } N \text{ is odd} \\ &\lambda_{N+2} = \tfrac{1}{8}, \ \ \lambda_{N+3} = \tfrac{1}{16}, \ \ \lambda_{N+4} = \tfrac{1}{32}, \ \ \lambda_{N+5} = \tfrac{1}{64} \end{aligned}$$

E Expressions of Φ_j's

All the Φ_j's defined in Section 8 can be analytically computed. Therefore, evaluation of a CCSS patch using eq. (**??**) is always possible no matter if the patch is extra-ordinary or regular. To get the expressions

of Φ_j's we need to define a set of function $f_j(\omega, k)$ first:

$$f_j(\omega,k) = \frac{\bar{\mathrm{S}}}{N} * \mathrm{Real} \begin{bmatrix} a_{\omega(0-t)}\mathrm{X}_\omega[0,j] \\ a_{\omega(0-t)}\mathrm{X}_\omega[1,j] \\ . \\ . \\ a_{\omega(N-1-t)}\mathrm{X}_\omega[1,j] \\ a_{\omega(0-t)}\mathrm{X}_\omega[2,j] \\ . \\ . \\ a_{\omega(N-1-t)}\mathrm{X}_\omega[2,j] \\ a_{\omega(0-t)}\mathrm{X}_\omega[3,j] \\ a_{\omega(0-t)}\mathrm{X}_\omega[4,j] \\ a_{\omega(0-t)}\mathrm{X}_\omega[5,j] \\ a_{\omega(0-t)}\mathrm{X}_\omega[6,j] \\ a_{\omega(1-t)}\mathrm{X}_\omega[3,j] \\ a_{\omega(1-t)}\mathrm{X}_\omega[4,j] \\ a_{\omega(1-t)}\mathrm{X}_\omega[5,j] \end{bmatrix} * \mathrm{X}_\omega^{-1}[j,s]$$

where $0 \le j \le 6$, $0 \le \omega \le \frac{N}{2}$, $\mathrm{Col} = \{0, N, N+1, \cdots, 3N-1, 3N, 4N, 5N, 6N, 3N+1, 4N+1, 5N+1\}$, $s = \mathrm{Col}[k]/N$, and $t = \mathrm{Col}[k]\%N$. When N is even and $\omega = \frac{N}{2}$,

$$f_j(\omega,k) = \begin{cases} (f_j(\omega,k) + f_{j+1}(\omega,k))/2, & j = 1 \\ f_j(\omega,k)/2, & j = 3,4,5,6 \end{cases}$$

Then we have

$$\begin{array}{lcl}
\Phi_0 & = & N[f_0(0,0), f_0(0,1), \cdots, f_0(0,2N), \mathbf{0}], \\
\Phi_{2j+1} & = & 2[f_1(j,0), f_1(j,1), \cdots, f_1(j,2N), \mathbf{0}], \\
\Phi_{2(j+1)} & = & 2[f_2(j,0), f_2(j,1), \cdots, f_2(j,2N), \mathbf{0}], \\
 & & j = 0,1,\cdots,2\lfloor\frac{N}{2}\rfloor + 1 \\
\Phi_{2\lfloor\frac{N}{2}\rfloor+2} & = & 2[f_2(\lfloor\frac{N}{2}\rfloor,0), f_2(\lfloor\frac{N}{2}\rfloor,1), \cdots, f_2(\lfloor\frac{N}{2}\rfloor,2N), \mathbf{0}], \\
 & & \text{if } N \text{ is odd} \\
\Phi_{N+2} & = & 2[\sum_l^{N/2} f_3(l,0), \sum_l^{N/2} f_3(l,1), \cdots, \\
 & & \sum_l^{N/2} f_3(l,2N), v_0] \\
\Phi_{N+3} & = & 2[\sum_l^{N/2} f_4(l,0), \sum_l^{N/2} f_4(l,1), \cdots, \\
 & & \sum_l^{N/2} f_4(l,2N), v_1] \\
\Phi_{N+4} & = & 2[\sum_l^{N/2} f_5(l,0), \sum_l^{N/2} f_5(l,1), \cdots, \\
 & & \sum_l^{N/2} f_5(l,2N), v_2] \\
\Phi_{N+5} & = & 2[\sum_l^{N/2} f_6(l,0), \sum_l^{N/2} f_6(l,1), \cdots, \\
 & & \sum_l^{N/2} f_7(l,2N), v_3]
\end{array}$$

where $\mathbf{0}$ is a row vector of 7 zeros and $v_k = (v_{k0}, v_{k1}, v_{k2}, v_{k3}, v_{k4}, v_{k5}, v_{k6})$.

References

[1] Austin SP, Jerard RB, Drysdale RL, Comparison of discretization algorithms for NURBS surfaces with application to numerically controlled machining, *Computer Aided Design* 1997, 29(1): 71-83.

[2] Ball AA, Storry DJT, Conditions for tangent plane continuity over recursively generated B-spline surfaces, ACM Transactions on Graphics, 1988, 7(2): 83-102.

[3] Ball AA, Storry DJT, An investigation of curvature variations over recursively generated B-spline surfaces, ACM Transactions on Graphics 1990, 9(4):424-437.

[4] Catmull E, Clark J. Recursively generated B-spline surfaces on arbitrary topological meshes, Computer-Aided Design, 1978, 10(6):350-355.

[5] DeRose T, Kass M, Truong T, Subdivision Surfaces in Character Animation, Proceedings of SIGGRAPH, 1998: 85-94.

[6] Doo D, Sabin M, Behavior of recursive division surfaces near extraordinary points, Computer-Aided Design, 1978, 10(6):356-360.

[7] Halstead M, Kass M, DeRose T, Efficient, fair interpolation using Catmull-Clark surfaces, Proceedings of SIGGRAPH, 1993:35-44.

[8] Reif U, A unified approach to subdivision algorithms near extraordinary vertices, Computer Aided Geometric Design, 1995, 12(2): 153-174.

[9] Sederberg TW, Zheng J, Sewell D, Sabin M, Non-uniform recursive subdivision surfaces, *Proceedings of SIGGRAPH*, 1998:19-24.

[10] Stam J, Exact Evaluation of Catmull-Clark Subdivision Surfaces at Arbitrary Parameter Values. *Proceedings of SIGGRAPH* 1998:395-404.